XI International Conference on Computational Plasticity. Fundamentals and Applications
COMPLAS XI
E. Oñate, D.R.J. Owen, D. Peric and B. Suárez (Eds)

NUMERICAL SIMULATION STUDY OF THE KNOOP INDENTATION TEST

M.I. SIMÕES[*], A.X. MARTINS[†], J.M. ANTUNES[*†], N.A. SAKHAROVA[†], M.C. OLIVEIRA[†] AND J.V. FERNANDES[†]

[*]Escola Superior de Tecnologia de Abrantes, Instituto Politécnico de Tomar
Rua 17 de Agosto de 1808, 2200 Abrantes, Portugal
e-mail: {isabel.simoes, jorge.antunes}@ipt.pt, web page: http://www.esta.ipt.pt

[†] CEMUC – Department of Mechanical Engineering, University of Coimbra,
Rua Luís Reis Santos, Pinhal de Marrocos, 3030-788 Coimbra, Portugal
e-mail: {marta.oliveira, nataliya.sakharova, valdemar.fernandes}@dem.uc.pt,
web page: http://www2.dem.uc.pt/cemuc/

Key words: Knoop Indentation, Ultramicrohardness, Numerical simulation.

Abstract. This paper presents a study of the influence of the mechanical properties of materials on the surface indentation geometry and on the depth-sensing indentation results with a Knoop indenter. Three-dimensional numerical simulations of this indention test were performed for several materials, with different mechanical properties, using the in-house finite element simulation code, DD3IMP. In order to obtain accurate results, the numerical model of the Knoop indenter was prepared, taking into account the optimization of the finite element mesh.

1 INTRODUCTION

Depth-sensing indentation tests have been employed like a standard technique for the mechanical characterization of bulk and composite materials. Experimental hardness tests are mainly performed using pyramidal Vickers and Berkovich indenters. The Knoop indenter differs from Vickers indenter merely in the indenter pyramid shape. The Knoop indenter geometry, with lozenge-based pyramid, leads to a more extended and shallower indentation impression than the Vickers indenter with square-based pyramid geometry. This makes the Knoop indentation attractive for determining the intrinsic thin film hardness [1] and for material anisotropy determination.

At our knowledge, studies of depth-sensing indentation using the Knoop indenter are unusual and further investigation is needed. Few examples are the experimental work conducted by Riester et al. [2, 3] and the numerical studies performed by Li Min *et al*. [4] and Giannakopoulos *et al*. [5].

Due to the scarce number of experimental and numerical studies, concerning the Knoop indenter, their enlargement could become very valuable in the characterization of some type of materials, such as thin films and anisotropic materials. In this context, the goal of the present study is to contribute for an improved understanding of the influence of the materials

mechanical properties on the indentation geometry and, consequently, on the mechanical properties evaluation by the Knoop hardness test.

2 THEORETICAL ASPECTS

The Knoop indenter has a pyramid-shaped geometry with apical angles of 130° and 172.5°, and a base with one diagonal, L, 7.11 times longer than the other, m, [6]. The Knoop indenter geometry is shown in Figure 1.

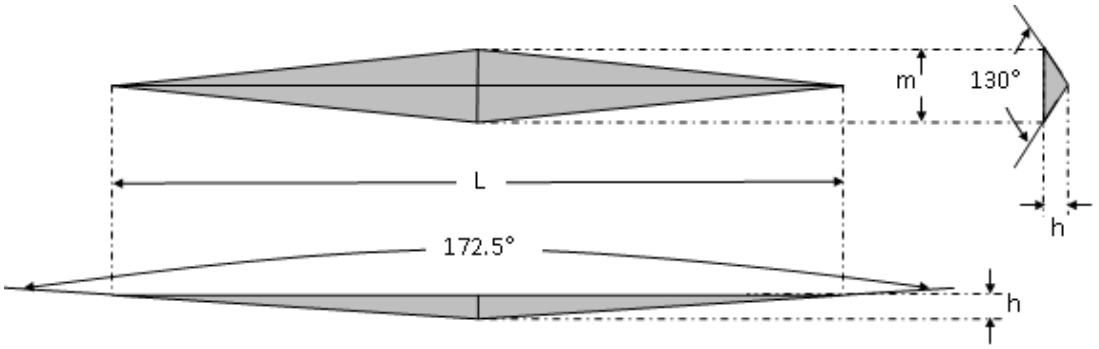

Figure 1: Geometry of the Knoop Indentation

The Knoop indenter contact area, A, as a function of the indentation depth, is given by:

$$A = 2h_c^2 \tan\theta_1 \tan\theta_2 = 65.4h_c^2, \quad (1)$$

where h_c is the indentation contact depth and θ_1=65°, θ_2=86.25° are the semi-apical angles of the indenter.

Marshall *et al.* [7] investigated the Knoop indentations and observed that, during the unloading period, the short diagonal of indentation (m) contracts, due to the elastic recovery, while the long diagonal (L) remains unchanged (see Figure 2).

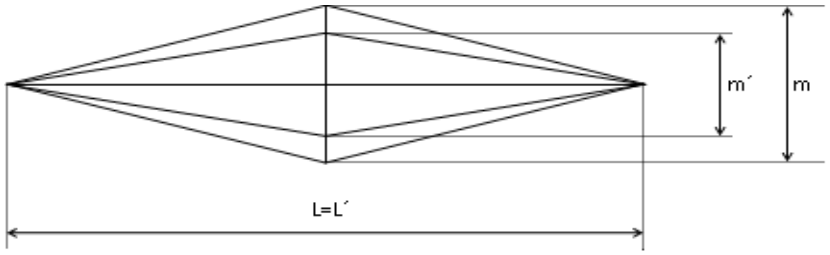

Figure 2: The short diagonal m reduces to m´, the long diagonal remains unchanged L=L´ after unloading

In the study of Marshall *et al.* [7], an equation for the recovered indentation size, which takes into account the indenter's geometry and the material mechanical properties, was proposed:

$$\frac{m'}{L'} = \frac{1}{7.11} - 0.45\frac{H}{E}, \quad (2)$$

where H is the hardness and E is the Young's modulus. Based on Marshall *et al.* [7] work, the

H and E values obtained by traditional methods are overestimated due to the substantial elastic recovery of the short diagonal compared with negligible elastic recovery of the long axis direction. In order to improve the mechanical properties results, an iterative procedure based in Equation (2) was proposed [7]: the initial values of H and E are calculated by the traditional methods and the ratio H/E is adjusted until convergence.

In this context, the aim of the current study is to investigate the Knoop indentation test. A detailed study concerning to the Knoop indentation surface geometry, at maximum load and after unloading, is performed. To attain this objective, three-dimensional numerical simulation of several fictitious materials was performed.

3 NUMERICAL SIMULATION AND MATERIALS

In order to perform the numerical simulations of the Knoop hardness test, the finite element DD3IMP in-house code was used. This code was developed to simulate processes involving large plastic deformations and rotations, considers the hardness tests a quasi-statistic process and makes use of a fully implicit algorithm of Newton-Rapson type [8,9]. The code allows the three-dimensional numerical simulations of the hardness test using any type of indenter geometry and takes into account the friction between the indenter and the deformable body. A detailed description of the DD3IMP simulation code has previously been given [10].

The test sample used in the numerical simulations of the indentation test has both radius and thickness of 40 μm. Figure 3 shows a global view and a detail of the indentation region of the finite element mesh. The discretization was performed using three-linear eight-node isoparametric hexahedrons. Due to geometrical and material symmetries in the X=0 and Z=0 planes, only a quarter of the sample was used in the numerical simulation of the Knoop hardness test. The finite element mesh was composed by 17850 elements. The mesh refinement was chosen in order to provide accurate values of the indentation contact area, and consequently of the mechanical properties.

In all the numerical simulations, the contact with friction between the indenter and the deformable body was considered, with a Coulomb's coefficient equal to 0.16 [10].

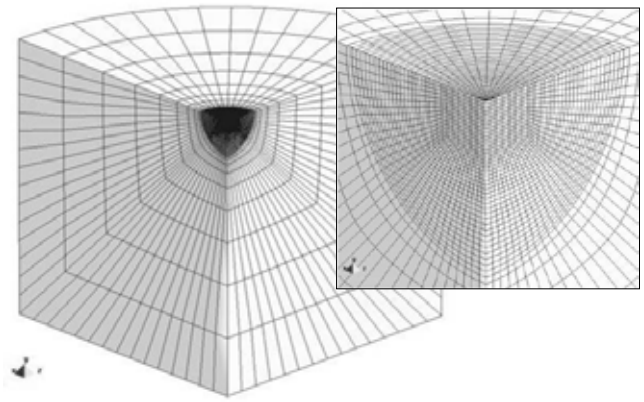

Figure 3: Finite element mesh for the test sample used in the numerical simulations.

The Knoop indenter geometry was modelled using parametric Bezier surfaces, which allow a fine description of the indenter tip, namely an imperfection such as the one that occurs in the real geometry, similar to the case of the Vickers indenter [11]. The model of the indenter has a tip imperfection, which consists in a plane normal to the indenters' axis with an area equal to 0.0032 μm^2. Figure 4 shows a global view of the Knoop geometry and a detail of the indenter tip.

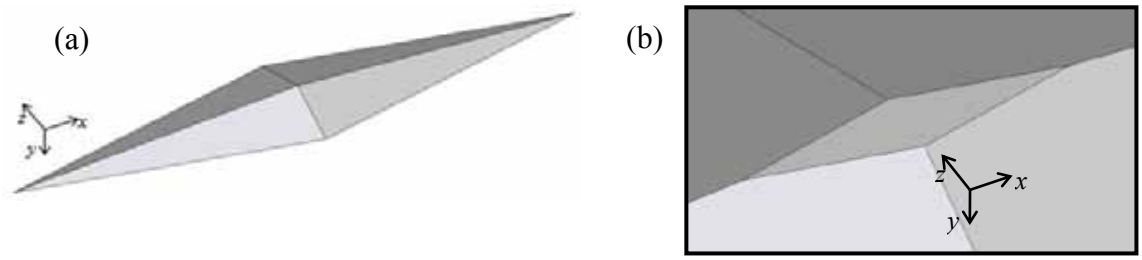

Figure 4: Knoop indenter modelled with Bezier surfaces. (a) general view; (b) detail of the indenter tip

Due to the tip imperfection, the indenter area function disagrees from the ideal. The following equation provides the Knoop indenter area function used in the analysis of the numerical results:

$$A = 65.4377h_c^2 + 0.9152h_c + 0.0032 \tag{3}$$

The numerical simulations of the Knoop hardness test were carried out on 10 fictitious materials, up to the same maximum indentation depth, $h_{max} = 0.2\,\mu m$. Table 1 resumes the mechanical properties of the materials considered. The plastic behaviour of the materials was modelled considering that the true-stress, σ, and the logarithmic plastic strain, ε, relationship was described by the Swift law: $\sigma = k(\varepsilon + \varepsilon_0)^n$, where k, ε_0 and n (strain hardening parameter) are material constants (the material yield stress is given by: $\sigma_y = k\varepsilon_0^n$). The constant ε_0 was considered to be 0.005 for all materials.

Table 1: Mechanical properties of the fictitious materials used in the numerical simulations

Material	σ_y (GPa)	n	E (GPa)	ν	h_f / h_{max}
M1	2	0.01	200	0.3	0.83
M2	10				0.49
M3	20				0.28
M4	2	0.3			0.70
M5	6				0.41
M6	20				0.15
M7	10	0.01	400		0.66
M8	20				0.49
M9	2	0.3			0.82
M10	20				0.24

3 RESULTS AND DISCUSSION

The fictitious materials considered (see Table 1) had two different Young' modulus (200 GPa and 400 GPa). Two different cases of work-hardening coefficient, n (on one side, the materials were assumed elastic-perfectly plastic (n ≈ 0) and by the other side, the materials had high work-hardening coefficient (n=0.3)), and different yield stress values σ_y were studied. In order to study the mechanical properties influence on the results of the Knoop indentation, the surface indentation profiles were analysed along both diagonals, the long diagonal, L, and the short one, m, as shown in Figures 5 and 6, respectively. Moreover, these figures show the indentation profiles at the maximum load (open symbols) and after unloading (solid symbols).

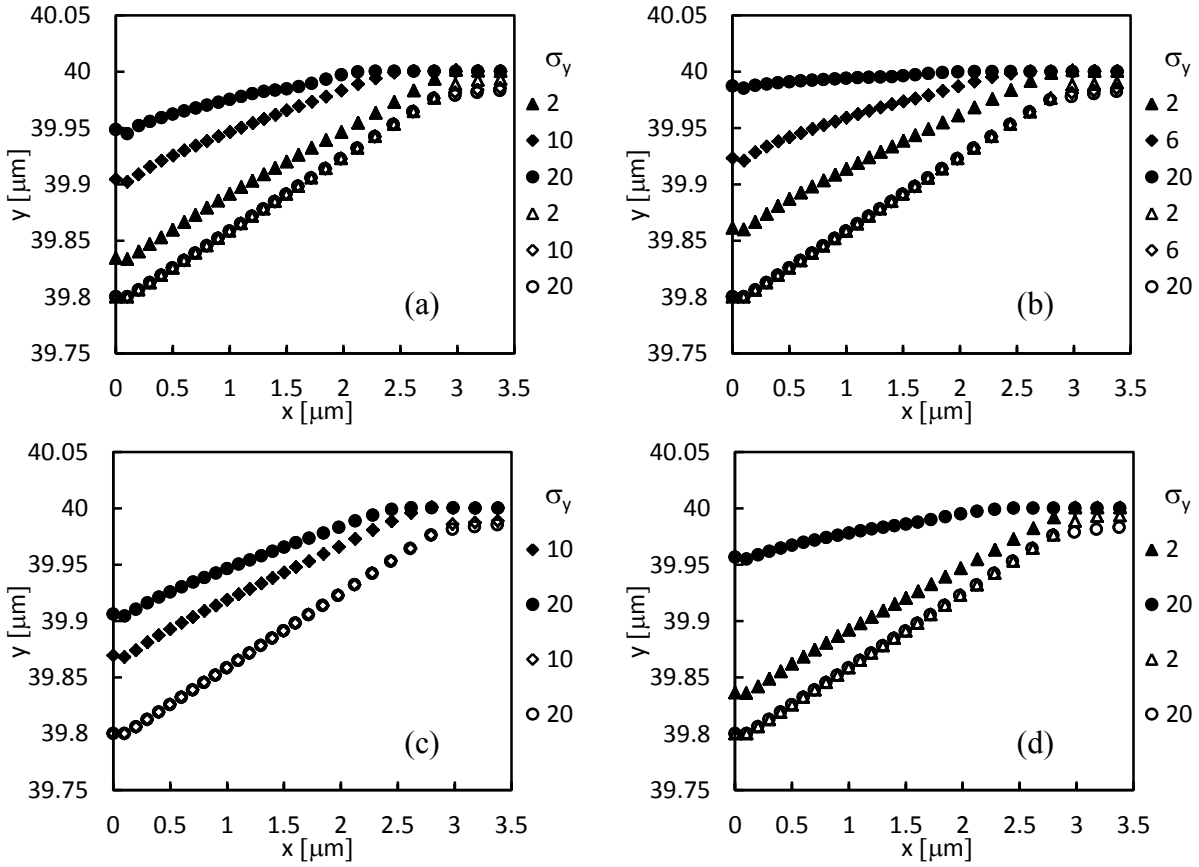

Figure 5: Surface indentation profiles at the maximum load along the longer diagonal, L, for the following materials: (a) M1, M2 and M3; (b) M4, M5, M6; (c) M7 and M8; (d) M9 and M10

Figures 5 and 6 show that the "sink-in" appears on the indentation surface at the maximum load, except in case of the M1 material, where the surface tends to form "pile-up". This fact certainly is related with a ratio h_f/h_{max} equal 0.83 (where h_f is the indentation depth after unload and, h_{max} the indentation depth at the maximum load) and the low value of the work-hardening coefficient. In fact, in case of Vickers indentation, the indentation profiles are related to the h_f/h_{max} ratio and the "pile-up" formation appears when this ratio is higher than

0.8, for low values of the work-hardening coefficient (n ≈ 0). So, the current results for the Knoop indentation are in agreement with previous studies for Vickers indenter [10]. It should be noted that, for a given material, the h_f/h_{max} ratio does not depends on the indentation depth and has a correlation with the value of the H/E ratio, between the hardness and the Young's modulus, which slightly depends on the work-hardening coefficient (the h_f/h_{max} ratio decreases when the H/E ratio increases).

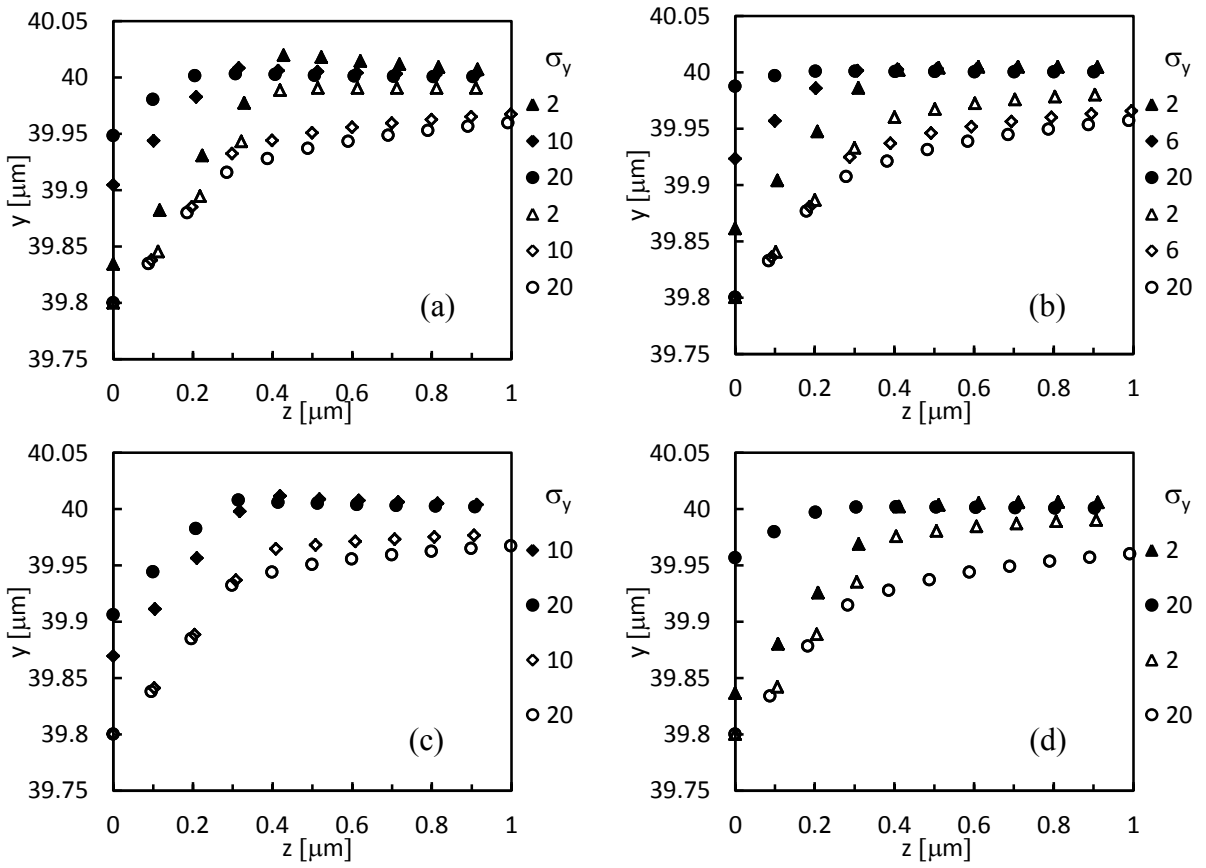

Figure 6: Surface indentation profiles at the maximum load along the short diagonal, m, for following materials: (a) M1, M2 and M3; (b) M4, M5, M6; (c) M7 and M8; (d) M9 and M10

After unloading, for materials with the same value of Young's modulus (E=200 GPa, Figures 5, 6 (a, b); E=400 GPa, Figures 5, 6 (c, d)), the surface indentation profiles show an elastic recovery along both diagonals that increases with the increase of the material yield stress, σ_y, and the work-hardening coefficient, n. Figures 5 and 6 also show that the increasing of the Young's modulus value leads to a decrease of the elastic recovery. Moreover, in the case of the short diagonal, for the materials M1 and M7, the indentation surface tends to form "pile-up". This is probably connected with the small elastic recovery.

As a general conclusion, the results presented in Figures 5 and 6 show that both indentation diagonals have elastic recover after unloading, as opposed to the conclusion by Marshall *et al*. [7]. In this context, the application of Equation (2) for the determination of the mechanical properties, namely the hardness and the Young's modulus, cannot be quite appropriate. This

becomes critical for materials with high work-hardening coefficient and higher values of the H/E ratio, between the hardness and the Young's modulus.

4 CONCLUSIONS

- This is an exploratory study concerning the numerical simulation of the Knoop indentation tests, in order to understand how to obtain accurate results concerning the mechanical properties of materials, namely the hardness and the Young's modulus;
- The surface indentation profiles shows "sink-in" formation for all materials except of ones with the h_f/h_{max} ratio slightly higher than 0.8;
- Elastic recovery for both diagonals of Knoop indentation is observed, although the elastic recovery along the short diagonal is inferior than the one along the long diagonal;
- The recovery along the indentation diagonals should be considered for determination of the mechanical properties by Knoop indentation test, especially for materials with high work-hardening coefficient and high ratio between the yield stress and Young's modulus; that is, it may be worth reexamining the use of the traditional equations for hardness and Young's modulus evaluation, providing that an adequate value of correction factor of indenter geometry is considered.

REFERENCES

[1] Chicot, D., Bemporad, E., Galtieri, Roudet, G. F., Alvisi, M. and Lesage, J. Analysis of data from various indentation techniques for thin films intrinsic hardness modelling. *Thin Solid Films* (2008) **516**:1964–1971.

[2] Riester, L., Blau, P. J., Lara-Curzio, E. and Breder, K. Nanoindentation with a Knoop indenter. *Thin Solid Films* (2000) **377-378**: 635-639.

[3] Riester, L., Bell, T.J. and Fischer-Cripps, A.C. Analysis of depth-sensing indentation tests with a Knoop indenter. *J. Mater. Res*. (2001) **16**:1660-1667.

[4] Li, M, Chen, W.M., Liang, N.G. and Wang, L.D. A numerical study of indentation using indenters of different geometry. *J. Mater. Res*. (2004) **19**: 73-78.

[5] Giannakopoulos, A.E. and Zisis, Th. Analysis of Knoop indentation. *Int. J. Solids Struct*. (2011) **48**:175-190.

[6] Knoop, F., Peters, C.G. and Emerson, W.B. A sensitive pyramidal-diamond toll for indentation measurements. J. *Res. Nat. Bur. Stand*. (1939) **23**:39–61.

[7] Marshall, D.B., Noma, T. and Evans, A.G. A simple method for determining elastic modulus to hardness ratios using Knoop indentation. *Int. J. Am. Ceram. Soc. A* (1982) **65**: C175–C176.

[8] Menezes, L.F. and Teodosiu, C. Three-dimensional numerical simulation of the deep-drawing process using solid finite elements. *J. Mater. Processing Technol.* (2000) **97**:100–106.

[9] M.C. Oliveira, J.L. Alves and L.F. Menezes, Algorithms and strategies for treatment of large deformation frictional contact in the numerical simulation of deep drawing process. *Arch. Comput Method* (2008) **E15**:113-162.

[10] Antunes, J.M., Menezes, L.F. and Fernandes, J.V. Three-dimensional numerical

simulation of Vickers indentation tests. *Int. J. Solids Struct.* (2006) **43**: 784–806.
[11] Sakharova, N.A., Fernandes, J.V., Antunes, J.M. and Oliveira, M.C. Comparison between Berkovich, Vickers and conical indentation tests: A three-dimensional numerical simulation study, *Int. J. Solids. Struct.* (2009) **46**:1095-1104.